Geophysical Research Letters / Volume 36, Issue 23

Oceans | Free Access

Observations of internal wave generation in the seasonally ice-free Arctic

Luc Rainville, Rebecca A. Woodgate

First published: 02 December 2009
https://doi.org/10.1029/2009GL041291

Abstract

[1] The Arctic is generally considered a low energy ocean. Using mooring data from the northern Chukchi Sea, we confirm that this is mainly because of sea-ice impeding input of wind energy into the ocean. When sea-ice is present, even strong storms do not induce significant oceanic response. However, during ice-free seasons, local storms drive strong inertial currents (>20 cm/s) that propagate throughout the water column and significantly deepen the surface mixed layer. The large vertical shear associated with summer inertial motions suggests a dominant role for localized and seasonal vertical mixing in Arctic Ocean dynamics. Our results imply that recent extensive summer sea-ice retreat will lead to significantly increased internal wave generation especially over the shelves and also possibly over deep waters. This internal wave activity will likely dramatically increase upper-layer mixing in large areas of the previously quiescent Arctic, with important ramifications for ecosystems and ocean dynamics.

1. Introduction

[2] The Arctic Ocean is a remarkably quiet ocean. It exhibits strong upper layer stratification, isolated bottom waters, and double-diffusive layering which is coherent across the Arctic [*Carmack et al.*, 1997]. These features exist because ocean mixing in the basins of the Arctic is much weaker than in most of the rest of the world oceans [*Rainville and Winsor*, 2008]. The primary reason for this quiescence is generally attributed to the dominant presence of sea-ice, which acts to isolate the ocean from the mixing effects of wind [*Padman*, 1995].

[3] Most of the transport in the Arctic Ocean (aside from in Fram Strait) is believed to be via sluggish boundary currents (order a few cm/s), coherent over most of the water depth and present over the slopes (500–3000 m isobaths [*Woodgate et al.*, 2001]). Velocities greater than

this are sometimes observed in eddies. These are believed to be important for transport of physical and biogeochemical properties from the boundaries to the interior of the deep basins, although their numbers and dynamics are relatively unknown [*Manley and Hunkins,* 1985; *Woodgate et al.,* 2001]. It has recently been suggested that double-diffusive driven layering, although only with mm/s scale velocities, is also currently a key mechanism for slope-to-deep-basin exchange [*McLaughlin et al.,* 2009].

[4] This paper considers another source of ocean energy – internal waves created by surface winds. Typically, wind blowing over the open ocean induces significant surface waves, inertial currents, and a deepening of the mixed layer, which entrains previously deeper water into the surface layer. Inertial internal waves are generated by these disturbances of the oceanic stratification. Internal waves (IW) can also be generated by interactions of tidal currents with rough topography. Unlike surface waves, IWs propagate vertically as well as horizontally. In the global ocean, deep mixing caused by IWs is believed to be critical in maintaining the meridional overturning circulation [*Munk and Wunsch,* 1998]. Locally, mixing processes that supply heat and nutrients from depth (>50 to 100 m) into the upper layers, especially the photic zone, will impact both the physical state of the Arctic (e.g., sea-ice formation) and Arctic biological systems.

[5] Measurements taken from ice stations have shown the energy level of the Arctic IW field is one to two orders of magnitude less than in other oceans [*Levine et al.,* 1985; *D'Asaro and Morison,* 1992; *Halle and Pinkel,* 2003]. Arctic tides are generally weak, ocean velocities are small, and the ice cover inhibits the transfer of momentum from the wind to the ocean, leading to much less IW generation [e.g., *McPhee and Kantha,* 1989]. Moreover, IWs are also strongly attenuated as they reflect off the ocean-ice interface [*Morison et al.,* 1985; *Pinkel,* 2005]. In the deep basins, measurements from ice-drifting camps or buoys suggest a seasonal variation in the strength of the IW field [*Plueddemann et al.,* 1998; *Halle and Pinkel,* 2003], although at least part of the observed variability is likely due to changes in camp/buoy location. On seasonally ice-free shelves, however, the role of IW for the evolution of the surface mixed layer and the erosion of the pycnocline is largely undocumented.

[6] In this paper, we present mooring observations of seasonal changes in IW energy level under varying sea-ice conditions at a fixed location. We consider 2-year mooring deployments in the northern Chukchi Sea, the large continental shelf sea joining the Bering Strait Pacific gateway with the Arctic Ocean (section 2). We show that when sea-ice is present, even strong storms do not induce significant oceanic response. However, during ice-free seasons, local storms drive strong inertial oscillations and IWs (section 3). The data suggest that vertical shear associated with inertial waves is responsible for deepening the surface mixed layer and enhancing vertical diffusivities in the entire water column (section 4). We discuss possible

implications of the dramatic contrast between the IW field with and without sea-ice for the current and future dynamics of the Arctic Ocean (section 5).

2. Observations

[7] As part of the NSF-SBI (Shelf Basin Interaction) program, two subsurface moorings (SBI3 and SBI4) were deployed by the University of Washington on the northern Chukchi Slope (Figure 1a) from July 2002 to September 2004, with mooring turnaround in September 2003 (for details, see http://www.eol.ucar.edu/projects/sbi). Mooring SBI3 (73° 20.3′ N, 166° 3.6′ W) was in 70 m of water and 30 km south of mooring SBI4 (73° 36.7′ N, 166° 2.5′ W), which was in 110 m of water. Both moorings carried upward looking RD Instruments 300 kHz Acoustic Doppler Current Profilers (ADCPs) at about 50 m depth recording hourly-averaged velocity in 2-m bins. Estimated uncertainties are usually less than 1 cm/s in speed and 1° in direction. Below the ADCPs, velocity data were recorded with Aanderaa RCM-7s at 55 m on SBI3 and 76 m on SBI4.

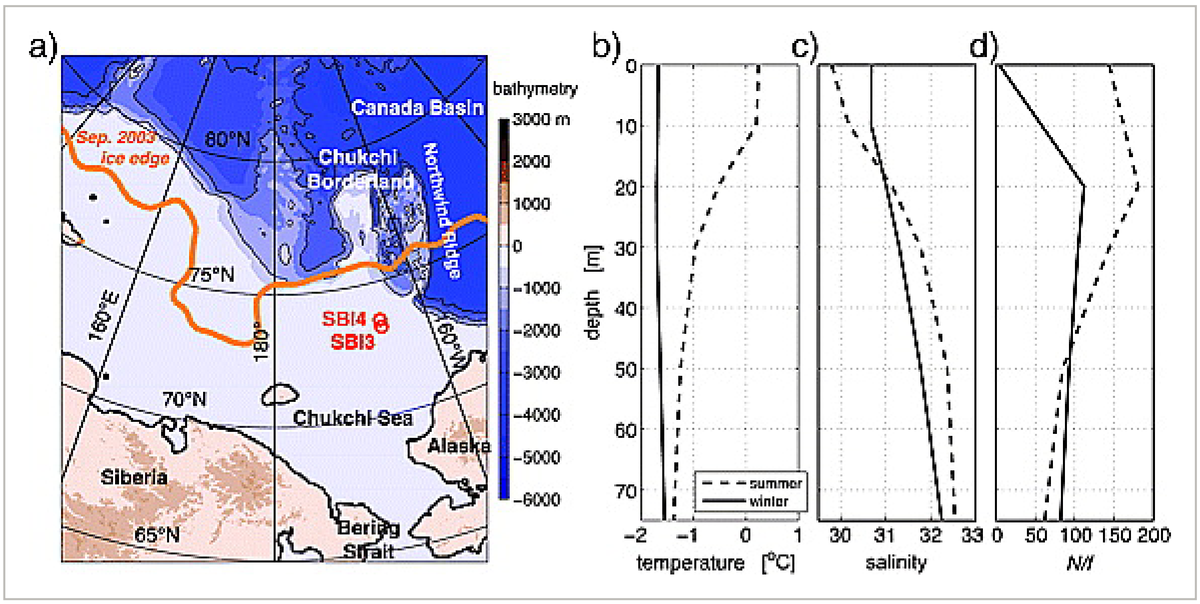

Figure 1

Open in figure viewer | PowerPoint

(a) Map of the Chukchi Sea showing the locations of the SBI3 and SBI4 moorings used in this study (open red circles). Colors and contours represent topographic data from IBCAO [*Jakobsson et al.*, 2008]. Average ice edge (20% ice concentration) for September 2003 is shown as the thick orange line. The ice edge in winter is south of Bering Strait. Climatological profiles of (b) temperature, (c) salinity, and (d) buoyancy frequency scaled by the local Coriolis parameter near the moorings, from the PHC3 [*Steele et al.*, 2001], showing averaged summer (dashed black) and winter (solid black) profiles.

[8] For our analysis, we use 10-m winds from the NCEP (National Centers for Environmental Prediction) Reanalysis project [*Kanamitsu et al.*, 2002] linearly interpolated from the 2.5° global NCEP grid to the mooring locations. The presence of sea-ice is determined from the echo

intensity of the ADCP surface return [*Shcherbina et al.*, 2005]. This estimate of ice-cover agrees well with the gridded sea-ice cover derived from satellite measurements (Special Sensor Microwave/Imager [SSM/I] product [*Cavalieri et al.*, 1996]). For reference, the location of the ice edge in September 2003 (annual minimum ice extent) estimated from satellite measurements is shown in Figure 1a.

[9] The barotropic tidal currents are estimated from the depth-averaged current data by fitting 8 tidal constituents to the 2-year time series of east and north velocity components. In general, tides are small - over the whole 2-year time-series, the barotropic tides account for 10–30% (less near the surface) of the total velocity variance for periods less than 2 days. The results (Table 1) agree well with a regional tidal assimilation model [*Padman and Erofeeva*, 2004], with differences possibly due to sea-ice effects and, for M_2, perhaps some small contribution from (incoherent) inertial motions. Overall, the total barotropic tidal currents rarely exceed 0.04 m s^{-1}.

Table 1. Amplitudes and Greenwich Phases (°G) of the Four Principal Barotropic Tidal Constituents at the SBI3 Mooring From Direct Observations and From a Regional Tidal Model [a]

Tidal Constituent	Eastward Barotropic Velocity				Northward Barotropic Velocity			
	Data		Model		Data		Model	
	[cm s^{-1}]	°G	[cm s^{-1}]	°G	[cm s^{-1}]	°G	[cm s^{-1}]	°G
M_2	2.7	138	1.9	137	2.8	050	2.1	049
S_2	1.1	168	1.1	173	1.2	079	1.1	089
K_1	0.4	002	0.8	7	0.4	244	0.3	219
O_1	1.2	353	1.0	27	1.1	248	0.4	269

a *Padman and Erofeeva* [2004]. Model results are interpolated to the mooring position and scaled by the actual depth.

[10] After the barotropic tides are removed, inertial velocities are extracted from both components of velocity at each depth by finding the magnitude and phase of the motion consistent with an oscillation rotating clockwise in time at the local inertial frequency, *f*, (corresponding to a period of 12.5 h) using a least-square fit over overlapping 2-day periods. Almost all (96 to 99%) of the velocity variance in the inertial frequency band is in the clockwise

component, and the resulting inertial oscillations represent between 30 and 60% of the total velocity variance for periods smaller than 2 days.

3. Inertial Waves and Seasonal Ice-Cover

[11] The wind speed time series at the mooring SBI3 (Figure 2a) shows that storms occur in all seasons at this location. The thick black bars in Figure 2 indicate periods when the sea-ice cover is estimated to be nearly 100% from the ADCP data. During ice-covered times, inertial oscillations are weak (less than 0.05 m s^{-1}) and show no obvious relationship to the overlying wind. The magnitude of these winter inertial motions is comparable to the values reported under ice by *Plueddemann et al.* [1998] during winter (inertial velocity amplitudes ~0.01 m s^{-1}). In contrast, when there is no ice, strong inertial currents, up to 0.30 m s^{-1}, are observed at the SBI sites (Figure 2b), larger than the 0.05–0.10 m s^{-1} summer amplitudes reported under ice above the Northwind Ridge [*Plueddemann et al.*, 1998]. The magnitude of the inertial oscillations is larger near the surface, but is also elevated in the whole water column.

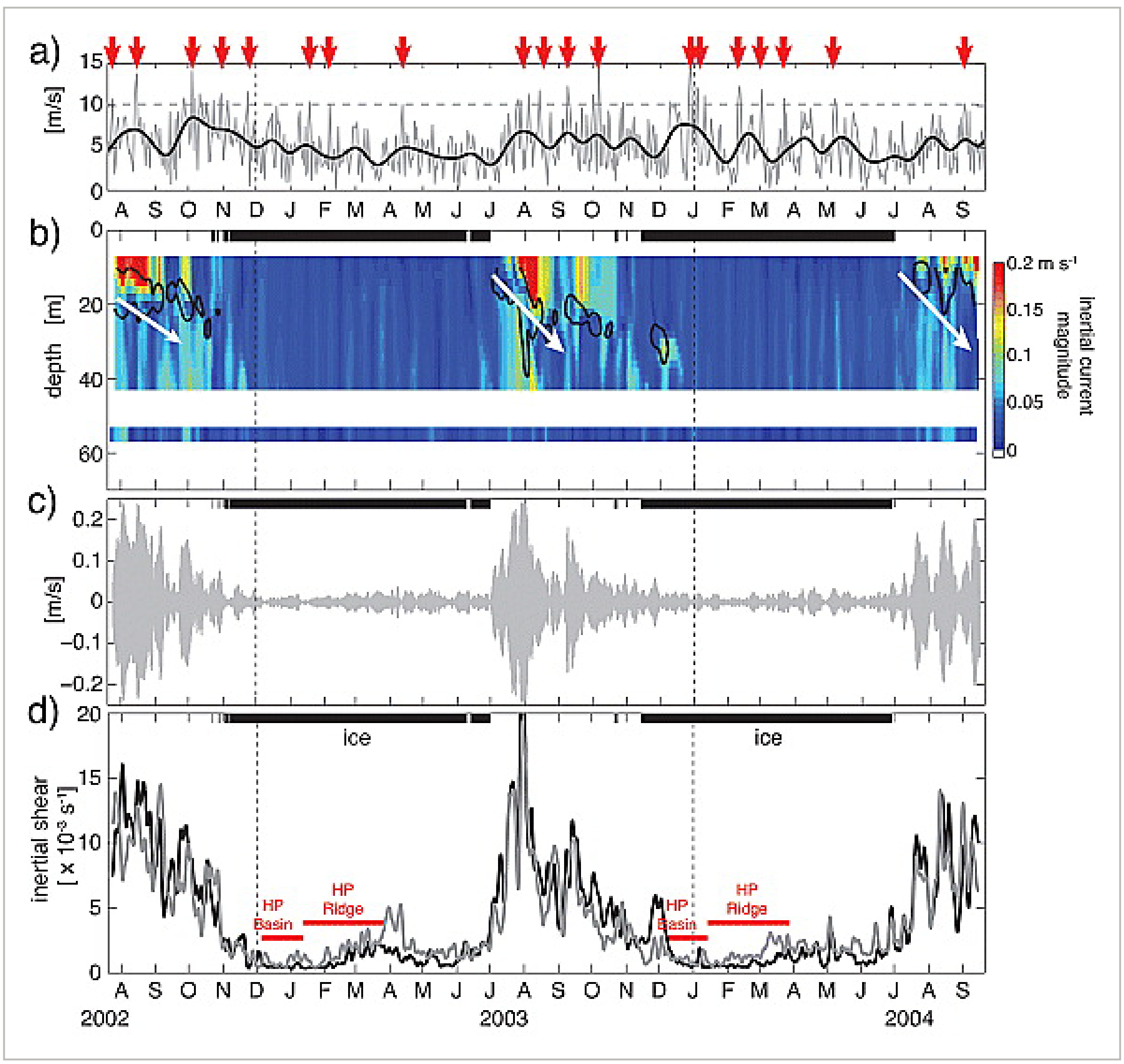

Figure 2

Open in figure viewer | PowerPoint

(a) Daily (gray) and 30-day running-mean (black) NCEP wind speed at the SBI3 mooring site. Red arrows indicate storms, defined as periods when daily wind speed exceeds 10 m s^{-1}. (b) Magnitude of the inertial currents at SBI3 as a function of depth and time, in m s^{-1}. Black contours indicate vertical shear $>10^{-2}$ s^{-1}. (c) Time series of the east component of the SBI3 inertial current at 10-m depth. (d) Time-series of inertial shear magnitude, calculated between 10 and 30 m and smoothed over 3 days, from ADCP data from SBI3 (black) and SBI4 (gray). Mean shear from the 1994 SIMI ice camp [*Halle and Pinkel*, 2003] is indicated by thin red bars. Thick black bars at the top of Figures 2b, 2c, and 2d indicate the presence of sea ice as derived from the ADCP data. White arrows are discussed in the text.

[12] It is possible that these internal waves are generated by the barotropic tide interacting with topography – waves that would be damped by under-ice reflections in winter but able to propagate in summer. However, the time series of inertial current and shear do not follow a spring/neap cycle associated with barotropic tidal forcing. Instead, strong inertial oscillations and strong vertical shear appear to be closely associated with each storm (Figure 2). We conclude that wind-generated inertial waves dominate the internal wave field during summer.

[13] The time-series of inertial shear, obtained from the vertical difference of velocity between 10 and 30 m, shows a large seasonal cycle (Figure 2d). The values measured in ice-free conditions are almost an order of magnitude greater than those obtained during winter. In the winter months (January, February, and March), the mean vertical shear between 10 and 30 m at both moorings is 1.2×10^{-3} s^{-1}, while the shear in the summer months (July, August, and September) averages to 8.3×10^{-3} s^{-1}. Decomposition of the shear into components rotating clockwise and counterclockwise with depth indicates that there is only a small excess of clockwise shear (53%) associated with downward propagating energy. This equipartition suggests multiple reflections.

[14] For comparison, the winter average at the SBI sites is about a factor of 2 smaller than the mean shear recorded during the 1993–1994 SIMI ice-camp in both the Canada Basin and above the Northwind Ridge [*Halle and Pinkel*, 2003]. Different ice conditions likely explain this difference. However, the SBI summer shear levels are much higher than previous Arctic observations. Even while the SHEBA ice camp was drifting over the Chukchi Borderland in summer 1998, the daily rms shear never exceeded 4×10^{-3} s^{-1} [*Pinkel*, 2005].

[15] At the SBI mooring sites, climatological data show that the water column is strongly stratified during the entire year (Figure 1d) - the buoyancy frequency below the surface mixed layer is always larger than ~10^{-2} s^{-1} (≈70f). Since we do not have year-round direct observations of the stratification, the depth of the maximum inertial vertical velocity shear (black contours in Figure 2b) is assumed a reasonable estimate of mixed layer depth [e.g., *Howard et al.*, 2004]. In association with large inertial currents and strong vertical velocity shear likely due to several

storms, the mixed layer is seen to grow rapidly during ice-free conditions (shown schematically by the white arrows). The deepest example is in summer 2003, where we infer that the mixed layer deepens to nearly 40 m. Thus, we conclude that summer IWs significantly erode the stratification of the pycnocline.

4. Estimation of Arctic Shelf Mixing

[16] Turbulence rates have been found to be very weak throughout the Arctic Ocean [*Rainville and Winsor*, 2008], with slightly elevated values in marginal seas and shelves [*Sundfjord et al.*, 2007]. A correlation has also been noted between bottom topography and IW shear, suggesting that most of the observed mixing is related to rough bottom topography [*D'Asaro and Morison*, 1992; *Dewey et al.*, 1999]. In contrast, a large part of the mixing in the world's oceans is believed to be associated with wind-generated IWs [*Munk and Wunsch*, 1998].

[17] An indirect estimate of the enhanced mixing due to IWs can be obtained from the magnitude of the IW shear measured at the mooring sites (Figure 2d). In the mid-latitude thermocline, diapycnal diffusivities have been found to be roughly proportional to the square of the vertical shear variance. The relationship derived by *Gregg* [1989] for the vertical diapyncal diffusivity, K, namely $K = K_0 V_z^4 \times {}_{GM}V_z^{-4}$, where $K_0 = 5.2 \times 10^{-6}$ m^2 s^{-1} is an empirical coefficient, V_z is the vertical shear, and ${}_{GM}V_z$ is the shear in the reference Garrett-Munk IW spectrum, gives us a first order estimate of the potential impact of the IW field. The assumption that diapycnal diffusivity is due to wave-wave interactions, embedded in *Gregg*'s [1989] parameterization, is unlikely to be justified on the shelves. Indeed, *Sundfjord et al.* [2007] found that this parameterization generally underestimates measured turbulent dissipation rates on the shelf of the Barents Sea. However, because of the lack of stratification and strain measurements in the upper water column, we cannot use perhaps more appropriate parameterizations [e.g., *MacKinnon and Gregg*, 2003].

[18] During the winter months, the low levels of vertical shear yield an averaged vertical diapycnal diffusivity of 2×10^{-7} m^2 s^{-1} in the pycnocline (10–30 m), smaller than the molecular diffusivities of heat and salt. This non-physical value suggests very little shear contribution to mixing processes during the winter and is consistent with the low mixing rates (10^{-6} m^2 s^{-1} and lower) measured in the central Arctic [*Rainville and Winsor*, 2008].

[19] In contrast, during the summer months, elevated shear values predict a dramatic increase in mixing, with an average (July, August, and September, 10 to 30 m) diapycnal diffusivity in the pycnocline of 2×10^{-4} m^2 s^{-1} and peak values above 1×10^{-3} m^2 s^{-1}. This estimate is larger than typical low-latitude thermocline values (~10^{-5} m^2 s^{-1} [*Gregg*, 1989]) and comparable with mixing hot spots (e.g., >10^{-4} m^2 s^{-1} at the Yermak Plateau [*Padman and Dillon*, 1991]) and shelf values at lower latitudes (~10^{-3} m^2 s^{-1} [e.g., *MacKinnon and Gregg*, 2003]).

5. Discussion of Implications for the Arctic Ocean

[20] It has been hypothesized that the dominant mixing of the Arctic Ocean occurs along the basin margins [*Padman*, 1995; *Pinkel*, 2005; *Timmermans et al.*, 2008]. The data presented here show that summer winds in ice-free regions generate strong inertial motions that deepen the surface mixed layer and erode the pycnocline. The mean vertical shear across the base of the surface mixed layer varies by an order of magnitude, from negligible in winter to ~0.01 s^{-1} in summer. Assuming that the dissipation rates and associated diapycnal diffusivities scale as shear, this implies much higher mixing rates in summer and that summer mixing dominates the annual average.

[21] Knowledge of the timing and the magnitude of the mixing associated with internal waves on the shelves is critical to understanding the Arctic Ocean and its likely ice-reduced future. About half of the Arctic Ocean has strong upper ocean stratification and subsurface layers of heat and nutrients at about 50-m depth of Pacific origin. The interplay of light, stratification and nutrient flux determines the success of photoplankton blooms, the base of the Arctic foodweb. Enhanced mixing, depending on timing, increases nutrient supply to the photic zone, or destroys the stratification necessary for productive success.

[22] Given the recent decreases in Arctic summer ice cover, these results suggest that IWs, and therefore wind-driven mixing, are likely to become more important at least on the shelves and probably also over the deep basin. Moreover, enhanced mixing in ice-free times will fundamentally change the heat storage in the upper layers with implications for sea-ice variability.

[23] It is still unclear what dynamics force the pan-Arctic circulation of Atlantic Water. *Zhang and Steele* [2007] found that, by changing mixing parameterizations in their coupled ice-ocean model from mid-latitude values to the weak values assumed for the Arctic Ocean, they could reverse the direction of Atlantic Water flow in the western Arctic (weaker mixing resulted in more cyclonic circulation). Moreover, there is increasing evidence that the double diffusive structures that are so ubiquitous to the Arctic [*Carmack et al.*, 1997] may be an integral part of mid-depth exchange between the Arctic Ocean boundary currents and the interior [*McLaughlin et al.*, 2009]. The velocity of these structures is 2 orders of magnitude less than the IWs we observe, and thus any significant wind-generated IW activity is likely to become a dominant mixing mechanism in the Arctic. It seems probable that a dramatic increase in mixing could fundamentally change pan-Arctic water transport and water mass transformations. This in turn would influence the Arctic's climate connections with the world ocean.

[24] Detailed modeling work is required to improve our understanding of how changes in ice cover will be reflected in changes in the spatial distribution of mixing rates in the Arctic Ocean,

and what consequences these will have for large scale hydrographic distributions. Quantified observations, such as hydrographic and microstructure measurements in different seasons and ice conditions, are essential to ground-truth predictions. We are perhaps about to experience a one-off experiment, the wind-driven spin-up of the Arctic Ocean.

Acknowledgments

[25] We thank Axel Schweiger for extracting the NCEP wind data and two anonymous reviewers for their helpful comments. Data were collected as part of the NSF-SBI program (ONR grant N00014-02-1-0305 and NSF grant OPP-0125082 for ship time), and our analysis supported by OPP-901438. We thank the Captain and crews of the USCGC Polar Star and Healy for dedicated work at sea. The SBI mooring data are freely available from http://psc.apl.washington.edu/HLD. Mooring and CTD data, and cruise details are available and are archived at JOSS/EOL.

Supporting Information

Filename	Description
grl26625-sup-0001-t01.txt plain text document, 611 B	Tab-delimited Table 1.

References

Carmack, E. C., K. Aagaard, J. H. Swift, R. W. Macdonald, F. A. McLaughlin, E. P. Jones, R. G. Perkin, J. N. Smith, K. M. Ellis, and L. R. Killius (1997), Changes in temperature and tracer distributions within the Arctic Ocean: Results from the 1994 Arctic Ocean section, *Deep Sea Res., Part II*, **44**, 1487– 1502, doi:10.1016/S0967-0645(97)00056-8 .

Cavalieri, D., C. Parkinson, P. Gloersen, and H. J. Zwally (1996), Sea ice concentrations from Nimbus-7 SMMR and DMSP SSM/I passive microwave data, digital media, Natl. Snow and Ice Data Cent., Boulder, Colo.